

Optimization of Inverse Snyder Polyhedral Projection

Erika Harrison
Department of Computer Science
University of Calgary
Calgary, Canada
eharris@ucalgary.ca

Ali Mahdavi-Amiri
Department of Computer Science
University of Calgary
Calgary, Canada
amahdavi@ucalgary.ca

Faramarz Samavati
Department of Computer Science
University of Calgary
Calgary, Canada
samavati@ucalgary.ca

Abstract—Modern techniques in area preserving projections used by cartographers and other geospatial researchers have closed forms when projecting from the sphere to the plane, as based on their initial derivations. Inversions, from the planar map to the spherical approximation of the Earth which are important for modern 3D analysis and visualizations, are slower, requiring iterative root finding approaches, or not determined at all. We introduce optimization techniques for Snyder’s inverse polyhedral projection by reducing iterations, and using polynomial approximations for avoiding them entirely. Results including speed up, iteration reduction, and error analysis are provided.

Keywords—equal area; projection; optimization

I. INTRODUCTION

Area preserving representations of the Earth’s surface have long been important. Research ranging from biological diversity studies, positional data regarding meteorological phenomena and the geographic spread of medical illnesses all rely on accurate area and regional information. Even business applications such as efficient regional marketing approaches and effective distribution techniques require such representation. Consequently, when working with data based on a spheroid shape, an approximation of our planet Earth, areal preserving projections become increasingly important.

As such it is imperative to preserve area when translating between a spherical representation of the Earth, to the planar layout upon which we view maps and process data. Such projections exist but often exhibit severe shape distortion. Snyder’s [1] polyhedral projection aims at reducing angular distortion, and has since been recommended for equal area projections [2]. The more recent Slice and Dice projection, presented by Leeuwen et al. [3], maintains areal preservation yet distributes angular distortion more uniformly. Transforming information from a planar representation to its spherical locality, or their inversions, is traditionally unimportant. In a Digital Earth framework, as proposed by former US Vice President, Al Gore [4], [5], this inverse process becomes extremely important since much underlying data is stored in a planar form. Geographic information systems (GIS), for example, employ such tactics to ensure enhanced accuracy of the data presented, enabling researchers with qualitatively improved methods for analysis.

Efficiency is also of the utmost importance. For example, a client analyzing bodies of water may require a thousand points to define the boundary of a lake from a coarse satellite image. If there were hundreds of lakes, as can be found in central Manitoba, this translates to over a million points that must be projected through this inversion process. Rivers, park boundaries and roads may also require simultaneous projection to meet the needs of modern businesses, military planners and scientific researchers. An effective approach must be taken to meet their real-time needs as experienced by geoscience visualization companies [6]. As such, a computationally and memory efficient approach for an inverse projection is desirable.

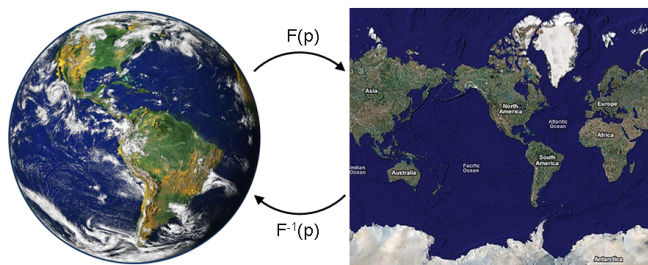


Figure 1. Projection from the Earth to Planar Map and Inverse (Right: Blue Marble, NASA [7], Left: Mercator Projection, Google Maps [8])

Traditional cartographic projections transform a point on the Earth to a point on a map. This projection can be described through a function:

$$p' = F(p),$$

where p is the point on the sphere, and p' is the resulting point on the map (Figure 1). Numerous projections have defined the function F , though not all are area preserving. These mathematical definitions are often constructed with this forward projection in mind. The inverse, or $F^{-1}(p)$ in Figure 1, defines the projection from the planar map to the spherical Earth. They are often derived directly from the forward projection.

Snyder’s equal area approach defines such a forward and inverse projection. His method is unusual in that it projects between a polyhedron, circumscribed within a sphere, and a

sphere, resulting in angular distortion greatly reduced from traditional single-plane map projections. Area is maintained by global and local preservation. Through a collection of trigonometric equations, the function $F(p)$ is described. The inversion, $F^{-1}(p)$, occurs as a direct reversal of the forward projection. From the trigonometric equations, a non-linear system evolves. Since neither Snyder nor traditional evaluations are able to construct an analytical or closed form, numerical solution finding is employed.

Due to this need for numerical solution finding, we see a drastic increase in calculation time. The closed form of the forward projection avoids this since it only computes the necessary calculations once. However, the iterative process from the solution finding repeats calculations and therefore increases the overall time. Since these iterations are applied for each call of the inversion, which in turn is called potentially millions of times for a single visualization, the process can slow down well below real-time requirements.

There are few other approaches for preserving area, while minimizing distortions. Leeuwen et al.'s Slice and Dice projection would offer a valid alternative, however it does not include an explicit definition of the inversion, let alone a computationally efficient approach.

The aim of our research is to optimize the inversion process employed by Snyder. In this way, it may be used in environments requiring real-time on-the-fly feedback. A variety of numerical and computational techniques are applied to improve the speed of the inversion. Repeated calculations are eliminated, efficient polynomial approximations are employed, and - most importantly - a reduction in the iterations of Newton's method is achieved. By evaluating data passed through the iterative process, an approximating curve can be extracted and used as an improved initial estimate, reducing our $F(p)$ to a one dimensional curve. This improved estimate reduces the time it takes to converge. An additional approach of applying the polynomial approximation directly, without requiring iterations is also explored.

We start with a detailed discussion on Snyder's equal area polyhedral projection, and its inversion. This is followed by the optimization techniques applied. These approaches are documented and their results presented, including speed ups, iteration reduction, and error analysis.

II. BACKGROUND

The Digital Earth framework, as proposed by former US Vice President, Al Gore [4], aims to increase the accessibility of data on the Earth's surface within a 3D spherical representation. This means that planar satellite images, field surveys and other such 2D data must be transformed from their planar locations to their respective spherical coordinates. Traditional features such as geographic boundaries, bodies of water, and transportation networks have been documented by cartographers in planar map form to facilitate discussion of such positional information. These projections,

from the Earth to the planar map, are wide and varied, spanning thousands of years [9].

One of the challenges faced by such projections is the inherent problem of transferring spherical data to a planar form. It is impossible to define a projection that preserves both the angles and area of features on the Earth. As such, projections are defined and chosen to be used according to the task required of them. Desirable characteristics include the preservation of area, preservation of shape, distance and positional accuracy, and an ease of computation [10]. With the advent of computers, this last characteristic - ease of computation - has become less critical to cartographers. Yet within a Digital Earth framework, requiring real-time analysis, computational complexity remains of high importance.

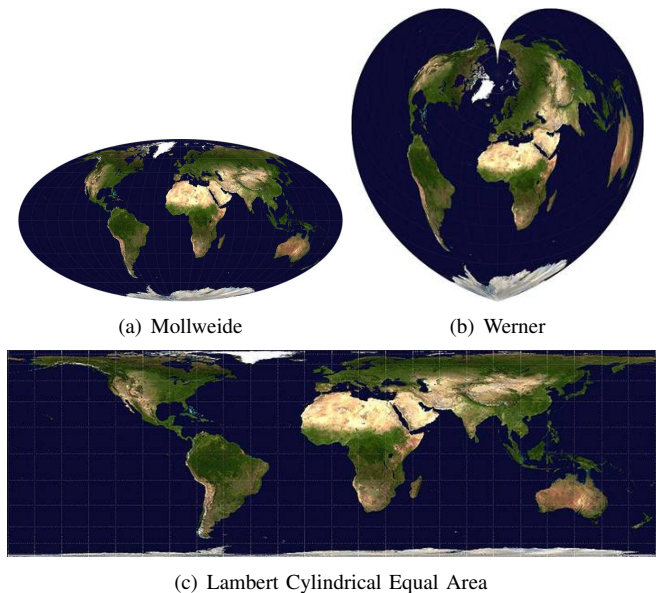


Figure 2. Area Preserving Projections (Blue Marble Series, NASA [7])

For researchers wishing to analyze features on the Earth, preservation of area is often required. Such projections have been documented since Ptolemy's *Geographia* manuscripts in the second century [9], with some incorporating other desirable projection characteristics. In some situations, attempting to retain distances as much as possible is desired, while in others, the overall shape (or angular) distortion should be minimized. The Werner projection [9] of the 16th century (Figure 2(b)), for example, generates a heart-shaped map, with a collection of distances preserved. However, shape distortion is extreme throughout the projection. The Lambert Equal-Area projections - azimuthal and cylindrical (Figure 2(c)) - are still commonly used today [11] [12]. They present the Earth's data over a more regular space, and while they reduce the distortion as seen in Werner's, the distance preservation is lost. The Mollweide projection [9] of the early 19th century (Figure 2(a)) retained areal equivalence while further improving the angular distortion

with its ellipsoidal shape. Despite these improvements, the angular distortion is still high at the boundaries and non-uniform across the planar mapping.

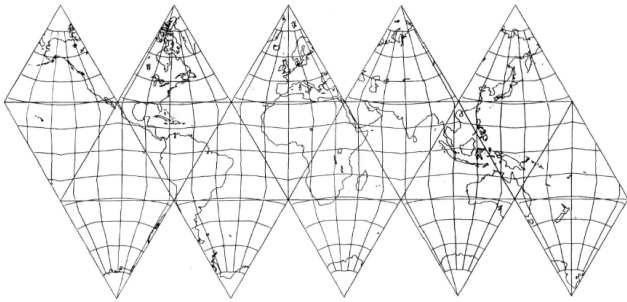


Figure 3. Icosahedral Mapping Using Snyder Equal Area Projection [1]

In projecting data for the Earth onto a sphere, Snyder [1] chose to use a polyhedral surface. As a result, angular distortion was greatly reduced due to the close approximation of the respective polyhedral shapes to that of a sphere. For example, with an icosahedron - illustrated in flattened form in Figure 3 - Snyder achieved an angular deformation of less than 17.3° and a scale variation of less than 16.3%. Further, this representation of a spherical world enables data on the polyhedron to be more easily managed in its flattened form before being visualized on the sphere.

Leeuwen et al. [3] later demonstrated an alternative areal preservation which distributes the angular deformation more uniformly across the surface of the projection. Their Slice and Dice approach explored areal calculations from a *derivative* approach. They start comparably to Snyder's projection, employing an initial polyhedral tessellation of the sphere, and reducing the problem to the smallest distinct region. From here, they divide the spherical triangle into four partitions, maintaining areal ratios en route. An intersection of these slices defines the position of the projected point. As a consequence, the distortions become less noticeable, eliminating discontinuities and reducing cusps. While their forward projection is defined - albeit fairly involved, requiring a dozen trigonometric calls - the inverse is not.

It should be noted that Song et al. [13] presented an equal area small circle subdivision. This subdivision divides triangles directly on the sphere into subtriangles using small circle arcs. For a single triangle, dozens of trigonometric calls ensure that all subtriangles are identical in area. While these faces could be indexed to their respective planar triangle, finding the projected location of a point would require repeated subdivision until the vertex of a subtriangle is sufficiently close to the point of interest. This approach is quite costly, especially when requiring numerous subdivisions to obtain high precision. As the objective of this paper is to compute an inverse projection quickly, Song's approach does not lend itself to a viable implementation.

III. EQUAL AREA POLYHEDRAL PROJECTIONS

A more detailed discussion of the Snyder polyhedral projection is explored. Its inversion is then presented, including notes pertaining to deficiencies in effective computation.

A. Snyder Projection

Snyder's projection defines a function F' which takes a point, p on the sphere, and determines its coordinates on a polyhedron. The main idea employs a modified Lambert Azimuthal Equal-Area projection, centering it respectively for each face. The modification corrects the otherwise imprecise edge matching between faces. Several steps define this projection. Firstly, the symmetric property of the polyhedral faces is recognized, and the problem is reduced to its smallest distinct region - always a right triangle (Figure 4). The second step ensures its area on the plane and on the sphere are equivalent through a scaling factor between the two radii. The third step generates a triangle on the polyhedron whose area exactly matches that of a spherical triangle bounded by point p . With this accomplished, the final step positions p' along this triangle's edge while maintaining areal scale.

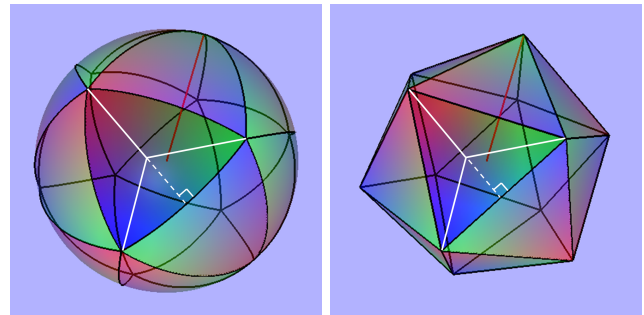


Figure 4. Spherical and Planar Icosahedron with Symmetric Decomposition (Red line indicates the radius)

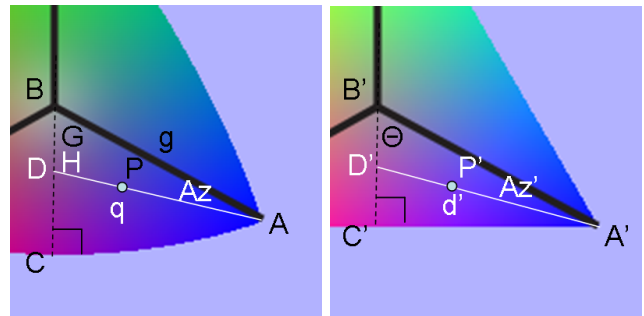


Figure 5. Snyder's Projection

Figures 4 and 5 illustrate the triangles and their variables. The initial extraction of the smallest distinct region is visualized in Figure 4, where the face is divided equally into three subtriangles, then further halved into a right triangle. This splitting may be applied to any regular polygon, which in

turn makes up the faces of the truncated icosahedron and the platonic solids - common sphere-circumscribing polyhedra.

Figure 5 illustrates several of the key angles and vertices used during the projection. The triangles $\triangle ABC$ and $\triangle A'B'C'$ represent the spherical and planar triangles of interest. These are associated with the underlying polyhedral face with A and A' the vertices, B and B' the centroids, and C and C' the midpoints along the edge. Our point of interest P is projected to P' using the projection. In the net-area preserving step, the radius R of the spherical polyhedron is associated with the radius R' of the sphere circumscribing the polyhedron. D is defined using a great circle arc from A through P , intersecting BC . The resulting triangle, $\triangle ABD$, with angles $\angle G$, $\angle H$ and $\angle Az$, is used to determine $\triangle A'B'D'$ with the same area. $\triangle A'B'D'$ need only be determined using the angle or azimuth $\angle Az'$, which may in turn determine the position of point D' . In the final step, the ratios between arc length $q = AD$ and edge length $d' = A'D'$ are used to position P' appropriately. It should be noted that due to the definition of the triangles, angles $\angle \Theta$ and $\angle G$ are fixed and known for the given polyhedron. These fixed values are found in Snyder's discussion [1].

With these terms defined, a discussion of Snyder's projection is readily facilitated. Recall the first step determines the approximate scaling factor between the radius R , of the sphere and the radius, R' of the sphere of which the polyhedron is circumscribed. This is uniquely determined for each platonic solid (and truncated icosahedron), and is based on areal calculations for the respective faces. For example, for the spherical triangle face, we observe that its area is:

$$A_{GT} = \frac{(G - \Theta)\pi R^2}{180^\circ}, \quad (1)$$

as defined through the spherical excess. The area of the planar triangle is computed using the traditional form, adjusting the width and height with respect to its circumscribing sphere. In this case, side $A'B' = R' \tan g$ and thus:

$$A_{MT} = \frac{1}{2}(R' \tan g)^2 \sin \Theta \cos \Theta. \quad (2)$$

Equating 1 and 2, and applying the numbers for the icosahedron, we achieve the scaling ratio of:

$$R' = 0.9104R,$$

which will ensure overall areal preservation.

The next step is to preserve localized areal equivalence. Recall that point D is formed by the intersection of great circle arcs AP and BC . Rather than computing D geometrically, one can use $\angle H$, calculated through the spherical Law of Sines and Cosines:

$$\angle H = \arccos(\sin Az \sin G \cos g - \cos Az \cos G). \quad (3)$$

This in turn defines the area of $\triangle ABD$ as:

$$A_{ABD} = \frac{(Az + G + H - 180^\circ)\pi R^2}{180^\circ}, \quad (4)$$

again through its spherical excess. To associate the area of $\triangle A'B'D'$ with its circumscribing radius, and angles of interest, Snyder defines the area as:

$$A_{A'B'D'} = \frac{(R' \tan g)^2 \tan Az'}{2(\tan Az' \cot \Theta + 1)}. \quad (5)$$

Since we need $A_{ABD} = A_{A'B'D'}$, we can transform equations 4 and 5 to define our planar azimuth, Az' :

$$Az' = \arctan(2A_{ABD}R'^2 \tan^2 g - 2A_{ABD} \cot \Theta).$$

The final step is to position point P' along this calculated azimuth, Az' so that it preserves overall areal scale. Snyder modifies the proportionality factor from the Lambert Azimuthal Equal-Area projection so that it complies with the polyhedral face. This proportionality factor becomes:

$$f = \frac{d'}{2R' \sin(q/2)}, \quad (6)$$

for arc length q and edge length d' . For any point at position z along the same azimuth Az' , one obtains the ratio:

$$\rho = 2R' f \sin(z/2), \quad (7)$$

which in turn is used to compute x , y on the planar face:

$$\begin{aligned} x &= \rho \sin Az', \\ y &= \rho \cos Az'. \end{aligned}$$

It should be noted that calculations presented by Snyder are reliant on the specific polyhedral layout and the x , y position and, latitude and longitude offsets for each polygon. These are visualized and listed within his paper. Employing these constants becomes a task in look up tables rather than generalizing for geometric shapes and points.

Though many trigonometric calls are required, this defines an effective closed form of the forward projection.

B. Inverse Snyder Projection

The inversion process finds the spherical coordinates of P given the polyhedral coordinates of P' . From the forward projection, we see that symmetric extraction and net areal scaling require nominal modification. In matching the areas of $\triangle ABD$ and $\triangle A'B'D'$, we have Az' and must compute Az . Thus, we can define the area of $\triangle A'B'D'$ as:

$$A_{A'B'D'} = \frac{R'^2 \tan^2 g}{2(\cot Az' + \cot \Theta)}.$$

Setting this equal to the area of $\triangle ABD$, from equation 4, we observe that Az is involved linearly and trigonometrically, through $\angle H$'s reliance on the arccos of $\sin Az$ and $\cos Az$ by equation 3. Solving for Az results in a non-linear equation. Since a closed form is neither proposed nor easily determined, Snyder suggests the Newton-Raphson iterative approach [1] to deduce an adequate value. This approach computes the derivative and uses it to iteratively find an improved approximate solution. We use the equations:

$$g(Az) = \frac{180^\circ A_{A'B'D'}}{\pi R^2} - G - H - Az + 180^\circ \quad (8)$$

$$g'(Az) = \frac{\cos Az \sin G \cos g + \sin Az \cos G}{\sin H} - 1 \quad (9)$$

$$\Delta Az = -\frac{g(Az)}{g'(Az)}$$

On each iteration, ΔAz is added to Az until ΔAz goes below some pre-determined threshold.

The final positioning of P along great circle arc AD is straightforward using the proportionality from equation 7.

Due to the non-linear equation, this inverse projection requires a number of iterations to converge on a value within a required accuracy. It should be noted that some of the computations within the iteration process are often repeated and therefore redundant within a formal implementation. These repetitions must be identified and removed.

IV. OPTIMIZATIONS

Since this inversion process has no known closed form, and requires iterative root-finding, numerous optimizations have been applied to speed up the calculations within iterations. In a graphical application where inversion calls occur millions of times within a single screen of information, slow implementations impede real-time requirements. While an order of magnitude in reduction is preferred, with such time costs even a constant reduction is beneficial.

Optimization of this inversion process has been applied to an icosahedron due to its numerous uniform triangular faces - a useful characteristic in computer graphics. Furthermore, the high face count reduces angular distortion from the projection. The optimizations described could also be applied to other sphere-circumscribing polyhedra, such as the platonic solids or truncated icosahedron.

Three types of optimizations are performed. Operation reduction, curve fitting and iteration removal are employed to speed up the inversion. While the most insightful optimization involves curve fitting for improved initial estimates, we start with operation reduction due to its simplicity.

A. Operation Reductions

A preliminary approach is recognizing repeated calculations - particularly within the iterative process - and pre-computing them. For example, $\cos Az$ and $\sin Az$ are used in the calculation of H , and again in calculating $g'(Az)$. In

turn, H is used in both $g(Az)$ and $g'(Az)$. These should only be computed once within the iteration. This is particularly meaningful given the additional time it takes to perform sine and cosine operations.

Storage of fixed values that are repeatedly employed will reduce the overall time. For example:

$$\frac{180^\circ A_{A'B'D'}}{\pi R^2} - G + 180^\circ \quad (10)$$

is fixed, yet used in the repeated calls to $g(Az)$. Instead it can be calculated once and used when necessary. Similarly $\sin G \cos g$ and $\cos G$, from $g'(Az)$, can be pre-computed. Other such repetitions, including the conversion between radians and degrees, can be simplified.

An additional speed up involves recognizing sine and cosine calls for the same angle, as occurs in equations 8, 9. For example, both $\angle G$ and $\angle Az$ require these calculations. Some compilers have a *sincos*, *sincosf* or *FSINCOS* directive to calculate these simultaneously in the time it takes to compute sine. Alternatively, an implementation such as Wanhammar et al.'s [14], could be employed.

B. Curve Fitting Numerical System

Ideally, we would like to avoid iterative solution finding. While a closed form would be preferable, one is neither proposed by Snyder nor readily deduced by standard solution-finding methods. An alternative is to analyze the iterative process. Notice how the result relies entirely on the input azimuth. For the angular range of the respective triangle (60° for an equilateral icosahedron face), we can plot the initial azimuth against the resulting azimuth, determined by the iterative root-finding process (Figure 6).

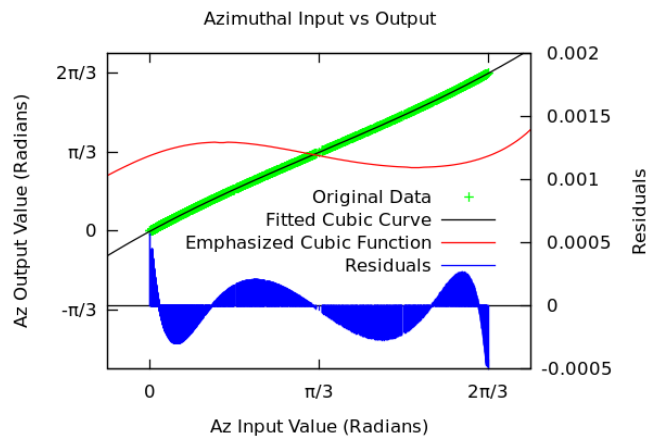


Figure 6. Azimuth Before Against Azimuth After Iterative Newton Raphson - Cubic Polynomial Approximation (Gnuplot 4.2)

Since the result is a smooth curve, it evokes the potential for a polynomial curve fitting approach. A cubic polynomial is fitted and visualized against the data to illustrate such a

tactic.¹ To emphasize its non-linear form, the exponential of its difference is plotted: $y = e^{5(f(x)-x)}$. The residuals of the data from this curve - scaled for visibility - are also shown. Curve fitting with higher order polynomials has been performed with residuals presented in Table I.

These polynomials can be used to provide an improved initial estimate for the iterative system. It is expected that convergence will occur faster as a result. Horner's Rule [15] will further ensure a minimization of operations.

Table I
POLYNOMIAL APPROXIMATING AZIMUTHAL SHIFT

Polynomial	Sum of Squares of Residuals	Variance of Residuals
Degree 1	1.19e+00	2.02e-04
Degree 2	9.27e-01	1.66e-04
Degree 3	2.30e-04	3.92e-08
Degree 4	2.06e-04	3.51e-08
Degree 5	2.51e-05	4.28e-09
Degree 6	2.20e-05	3.75e-09
Degree 7	9.06e-07	1.55e-10

C. Iteration Removal

Rather than improving the initial estimate, the polynomial could be evaluated for the definitive azimuthal value. In this way, we would use the result of the polynomial and skip the iterative calculations entirely. As such, the computations will change from:

```
Az ← poly(Az) // initial approximation
δ ← 1
while δ > 0 do
  δ ← F(Az)/F'(Az)
end while
```

to simply:

```
Az ← poly(Az)
```

Observe that a point projected with the iterative approach, and a point projected with this eliminated iteration will not coincide. If the offset is within a desirable precision, this error may be classified as negligible. Analysis of the positional and areal change will be necessary during validation.

V. RESULTS

Implementation and testing occurred using Qt/C++ on an Intel i7 quad core processor under Ubuntu 10.05.

The original implementation was contrasted against approaches described using the fitted cubic polynomial. While basic operation reduction is useful, comparison is not performed due to the inherent understanding that it will indeed speed up the calculations. Of more importance is the speed up of either a) reducing the iteration count through an improved initial estimate, or b) eliminating the iterative process by wholly using the polynomial approximation. For

¹At the expense of additional operations, Chebyshev polynomials [15] can be used. These will maintain stability in higher order polynomials.

the latter approach, an error analysis for areal change and displacement is also provided.

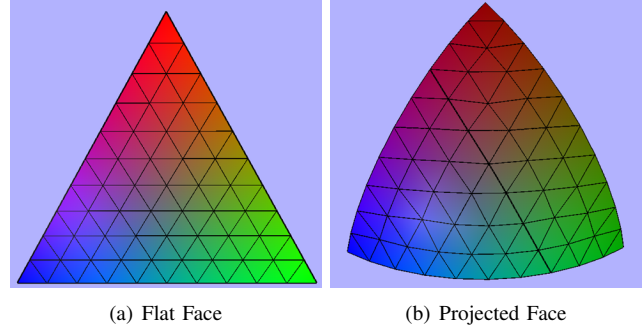


Figure 7. Quality 10 of Triangulated Face

For each of the three approaches - the original, improved polynomial approximation, and iteration elimination - profiling, using *gprof* (v2.17), was performed 100 times for four resolution, or quality levels. A resolution refers to the number of times an icosahedron face is initially divided prior to vertex projection. For example, a 10x10 resolution generates 100 triangles (Figure 7) whereas a 100x100 resolution will split the face into 10,000. Resolution levels 25, 50, 75 and 100 were profiled, with each region representing 4,080km², 1020km², 453km² and 255km² respectively on the Earth.

Table II
PROFILING RESULTS

Method. Quality	Avg Iter.	Avg Time (s)	Std Dev.	Time Improv.	Iter Improv.
O.25	3.61	0.0082	0.0083		
B.25	2.76	0.0059	0.0081	28.05%	23.66%
E.25	0	0.0035	0.0058	57.32%	
O.50	3.70	0.0229	0.0149		
B.50	2.82	0.0205	0.0131	10.48%	23.83%
E.50	0	0.0138	0.0113	39.74%	
O.75	3.74	0.0546	0.0222		
B.75	2.81	0.0509	0.0217	6.78%	24.72%
E.75	0	0.0310	0.0167	43.22%	
O.100	3.75	0.0996	0.0329		
B.100	2.83	0.0832	0.0292	16.47%	24.50%
E.100	0	0.0524	0.0209	47.39%	

Numerical results are presented in Table II. Column "Method.Quality" indicates the method - original (O), better approximation (B), eliminated iterations (E) - and quality level. The average iteration reflects the change in iteration distribution (Figure 8) as the quality improves, due to the increase of interior calls. Notice especially with lower qualities, that the standard deviation has the same order of magnitude as the average method time. For higher qualities, the results become more statistically significant. The percent time improvement compares the improved and eliminated approaches against the original. Iteration improvement over the original is presented for the improved but not the eliminated approach as no iterations occur.

Error analysis for the elimination approach can be found in Table III. Here, distance is an absolute value (Figure 9(b)). Given a point projected using the original inverse Snyder and the same point projected using the eliminated approach the distance error reflects the absolute displacement between the two points. For example, the average distance error of $9.379E-05\%$ is the equivalent of 5.903 m , based on an average Earth radius of $6,369\text{ km}$. The areal error is calculated using a quality-based triangle (Figure 9(a)). The error computes the triangle's change in area from its original to its eliminated projection. As the quality increases - and the size of the quality-based triangles decrease - the error also decreases. For example, at quality 100, the average error of $1.758E-06\%$ equates to 713.5 m^2 on the Earth.

Table III
ERROR ANALYSIS OF ELIMINATION APPROACH

Quality	Avg Dist. Error	Max Dist. Error	Avg Area Error (%)	Max Area Error (%)
25	9.379e-05	6.193e-04	1.982e-05	1.596e-02
50	9.439e-05	6.193e-04	9.223e-06	2.195e-02
75	9.459e-05	6.193e-04	3.330e-06	3.504e-02
100	9.490e-05	6.193e-04	1.758e-06	5.073e-02

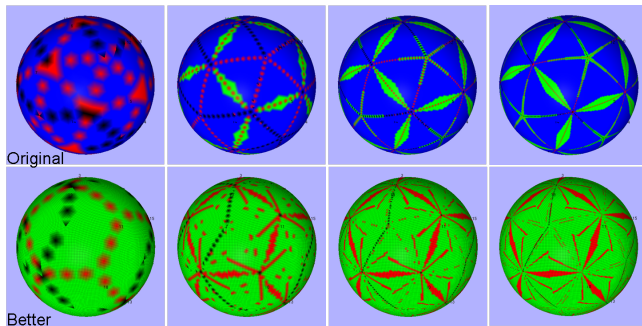
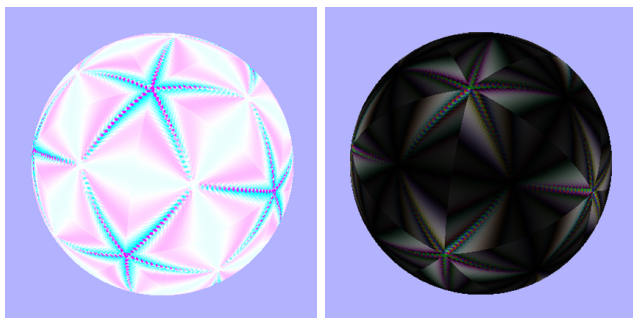


Figure 8. Iteration Distribution. (l-r) Quality 10, 30, 60, 100. Blue = 4, Green = 3, Red = 2, Black < 2



(a) Areal Change. Cyan - growth, Magenta - reduction (b) Distance Change. RGB associated with XYZ displacement

Figure 9. Visualization of Skip Distortions

VI. DISCUSSION

Based on the error comparison between the original projection and the eliminated approach, as illustrated in Table III, distance and areal errors are marginal. For example, with a resolution level of 100, the displacement equates to a mere 5.9 m , and an areal change of 0.7 km^2 . If these distances are indistinguishable from the visualization scale, it may be preferable to use this faster projection. If precision is of the utmost importance, with an error less than this eliminated approach, then the iteration reduction technique offers a viable alternative, reducing computation time by approximately 15%.

While a cubic polynomial was explored, a higher degree polynomial may be alternatively employed improving the approximation. This improved initial estimate reduces the number of iterations required to converge. A separate trial using a seventh degree polynomial resulted in 45% fewer iterations, as compared with the cubic. When this higher degree approximating polynomial was applied directly, vis-a-vis the eliminated approach, the areal and distance errors were reduced by a factor of 10. This equates to a distance error of 0.59 m on the Earth's surface, as compared with the cubic polynomial's 5.9 m . Notice that the seventh degree polynomial requires 14 operations to compute, whereas the cubic polynomial requires only 6 - both significantly less than the calculations in a single iteration. Consequently, when speed is of the essence, employing the eliminated approach with a cubic polynomial will prove fastest and fairly efficient. If speed and accuracy are important, a higher degree polynomial to better approximate the azimuth may prove more effective. The level of precision, amount of acceptable error and need for faster calculations must be considered when selecting the appropriate approach and polynomial.

VII. CONCLUSION

For large visualization systems that require real-time accurate and equal area information, an effective projection mechanism is critical. With modern data acquired through planar forms, preserving area during spherical conversion is of the utmost importance. This area preserving quality assists researchers and businesses with accurate analysis of the respective data (Figure 10 illustrates our improved implementation of the inverse Snyder projection, where, for example, Greenland has the same area on the icosahedron as on the sphere). Yet this analysis, along with the visualization, relies on underlying feature outlines which may span thousands or even millions of points for a single region. Converting these feature points into their spherical coordinates becomes an exercise in accuracy and speed. Frequent use of the inverse Snyder projection, as occurs in industry, can be very time consuming to the point of limiting the system. Any form of speed up assists in achieving the real-time qualities expected by modern clients.

The largest limiting factor in the inverse Snyder projection is the non-linear calculations of the azimuth, requiring iterative root-finding. A polynomial function may improve this by providing a more accurate initial estimate. For a cubic polynomial, this reduces the iterations by 25%. A seventh degree polynomial further improves this by 45%. For the cubic polynomial, this results in a 15% reduction in time spent performing the inversion, which in turn enables 15% more projections within a restricted real-time environment. Though iterations are reduced, this improved estimate still converges to an accurate azimuth, as per Snyder's approach.

An additional speed up may be achieved by using the polynomial to directly represent the azimuth. For the cubic polynomial, this results in a 47% reduction in time. In exchange for this large decrease, inherent errors occur. A higher degree will reduce the error at the expense of its own increased calculations. For the cubic polynomial, a displacement of 5.9 *m* results, whereas a seventh degree polynomial will decrease this by a factor of 10. While this error may be undesirable, for primitive visualizations or calculations, this faster approach may be beneficial.

While we tend to consider the Earth as a perfect sphere, gravitational forces make it thicker around the equator, and geological features leave it uneven. Incorporating these into our otherwise sufficient model demonstrates the fallibility of the area preserving approach taken. Given these non-spherical qualities, it would be of value to consider a multi-resolution areal preservation that takes into consideration the precise and imperfect shape of our home planet.

ACKNOWLEDGMENT

This work has been partially supported by PYXIS Innovation and NSERC. We would like to thank Idan Shatz for his thoughtful discussions.

REFERENCES

[1] J. P. Snyder, "An Equal-Area Map Projection for Polyhedral Globes," *Cartographica*, vol. 29, no. 1, pp. 10–21, 1992.

[2] A. J. Kimerling, K. Sahr, D. White, and L. Song, "Comparing Geometrical Properties of Global Grids," *Cart. and Geog. Information Science*, vol. 26, no. 4, pp. 271–288, Oct 1999.

[3] D. van Leeuwen and D. Strebe, "A Slice-and-Dice Approach to Area Equivalence in Polyhedral Map Projections," *Cartography and Geographic Information Science*, vol. 33, no. 4, pp. 269–286, 2006.

[4] A. Gore, "The Digital Earth: Understanding our Planet in the 21st Century," California Science Center. Los Angeles, CA, 31, Jan 1998.

[5] M. F. Goodchild, "Discrete Global Grids for Digital Earth," in *Proceedings of 1st International Conference on Discrete Global Grids*, March, 2000, 2006.

[6] PYXIS Innovation Inc, "How PYXIS Works," http://www.pyxisinnovation.com/pyxwiki/index.php?title=How_PYXIS_Works, 2011, [Accessed: May 1, 2011].

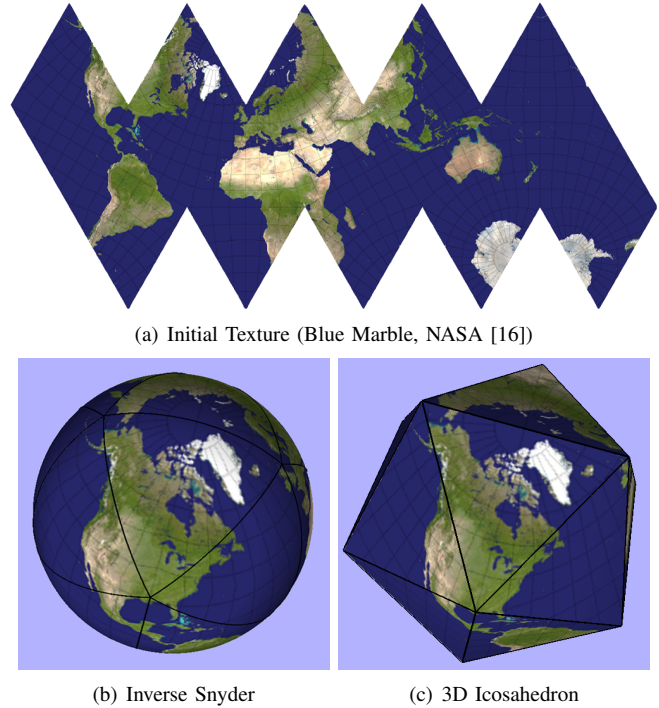


Figure 10. Inverse Snyder Projection

[7] NASA, "Blue Marble," <http://visibleearth.nasa.gov/>, 2000, [Accessed: Dec 11, 2010].

[8] Google - Imagery, "Google Maps," <http://maps.google.ca>, 2010, [Accessed: Dec 11, 2010].

[9] J. P. Snyder, *Flattening the Earth: Two Thousand Years of Map Projections*. Chicago, IL: Univ. of Chicago Press, 1997.

[10] —, *Map Projections - A Working Manual: U.S. Geological Survey Professional Paper 1396*. Washington, DC: U.S. Government Printing Office, 1987.

[11] Comm. for Environmental Cooperation, "North America," http://atlas.nrcan.gc.ca/site/english/maps/archives/various/north_america_cec, 2004, [Accessed: May 1, 2011].

[12] U.S. Dept. of the Interior, "Map Projections: From Spherical Earth to Flat Map," http://www.nationalatlas.gov/articles/mapping/a_projections.html, 2011, [Accessed: May 1, 2011].

[13] L. Song, A. J. Kimerling, and K. Sahr, *Discrete Global Grids*. Natl. Center for Geog. Information and Analysis, ch. Developing an Equal Area Global by Small Circle Subdivision.

[14] L. Wanhammar, K. Johansson, and O. Gustafsson, "Efficient Sine and Cosine Computation Using a Weighted Sum of Bit-Products," in *Proceedings of the 2005 European Conference on Circuit Theory and Design*, 2005.

[15] P. Borwein and T. Erdlyi, *Polynomials and Polynomial Inequalities*. New York, NY: Springer-Verlag, pp. 8–41.

[16] C. A. Furuti, "World Map on Icosahedron - Gnomonic," <http://www.progonos.com/furuti>, 2004, [Accessed: May 1, 2011].